CORRECTED 2 JULY 2010; SEE LAST PAGE

Bose-Einstein Condensation in Microgravity

T. van Zoest,[1] N. Gaaloul,[1] Y. Singh,[1] H. Ahlers,[1] W. Herr,[1] S. T. Seidel,[1] W. Ertmer,[1] E. Rasel,[1]* M. Eckart,[2] E. Kajari,[2] S. Arnold,[2] G. Nandi,[2] W. P. Schleich,[2] R. Walser,[3] A. Vogel,[4] K. Sengstock,[4] K. Bongs,[5] W. Lewoczko-Adamczyk,[6] M. Schiemangk,[6] T. Schuldt,[6] A. Peters,[6] T. Könemann,[7] H. Müntinga,[7] C. Lämmerzahl,[7] H. Dittus,[7] T. Steinmetz,[8] T. W. Hänsch,[8] J. Reichel[9]

Albert Einstein's insight that it is impossible to distinguish a local experiment in a "freely falling elevator" from one in free space led to the development of the theory of general relativity. The wave nature of matter manifests itself in a striking way in Bose-Einstein condensates, where millions of atoms lose their identity and can be described by a single macroscopic wave function. We combine these two topics and report the preparation and observation of a Bose-Einstein condensate during free fall in a 146-meter-tall evacuated drop tower. During the expansion over 1 second, the atoms form a giant coherent matter wave that is delocalized on a millimeter scale, which represents a promising source for matter-wave interferometry to test the universality of free fall with quantum matter.

The gedanken experiment of a freely falling elevator was crucial for the development of the theory of general relativity (GR) (*1*). In such an environment, there are locally no gravitational forces, an idea that gave birth to the equivalence principle. Whereas GR rules the macroscopic world, quantum mechanics (QM) dominates the microscopic scales and reveals the wave nature of matter. Bose-Einstein condensates (BECs) (*2*, *3*) exist on the border between quantum and classical physics; they are governed by the laws of QM but can take macroscopic dimensions. We took advantage of the absence of gravity in a freely falling elevator to follow the long-time (1-s) evolution of a BEC. In particular, we report the preparation and observation of a BEC during free fall in the 146-m-high drop tower of the Center of Applied Space Technology and Microgravity (ZARM) in Bremen, Germany, reaching expansion times up to 1 s that are difficult to reach in Earth-bound laboratories. The extended time of free fall allows us to observe the ultraslow expansion of the released BEC to a

[1]Institut für Quantenoptik, Leibniz Universität Hannover, Welfengarten 1, 30167 Hannover, Germany. [2]Institut für Quantenphysik, Universität Ulm, Albert Einstein Allee 11, 89081 Ulm, Germany. [3]Institut für Angewandte Physik, Technische Universität Darmstadt, Hochschulstrasse 4A, 64289 Darmstadt, Germany. [4]Institut für Laser-Physik, Universität Hamburg, 22761 Hamburg, Germany. [5]Midlands Ultracold Atom Research Centre, Birmingham B15 2TT, UK. [6]Humboldt-Universität zu Berlin, Hausvogteiplatz 5-7, 10117 Berlin, Germany. [7]Center of Applied Space Technology and Microgravity (ZARM), Universität Bremen, Am Fallturm, 28359 Bremen, Germany. [8]Max-Planck-Institut für Quantenoptik and Sektion Physik der Ludwig-Maximilians-Universität, Schellingstrasse 4, 80799 München, Germany. [9]Laboratoire Kastler-Brossel de l'Ecole Normale Supérieure, 24 rue Lhomond, 75231 Paris, France.

*To whom correspondence should be addressed. E-mail: rasel@iqo.uni-hannover.de

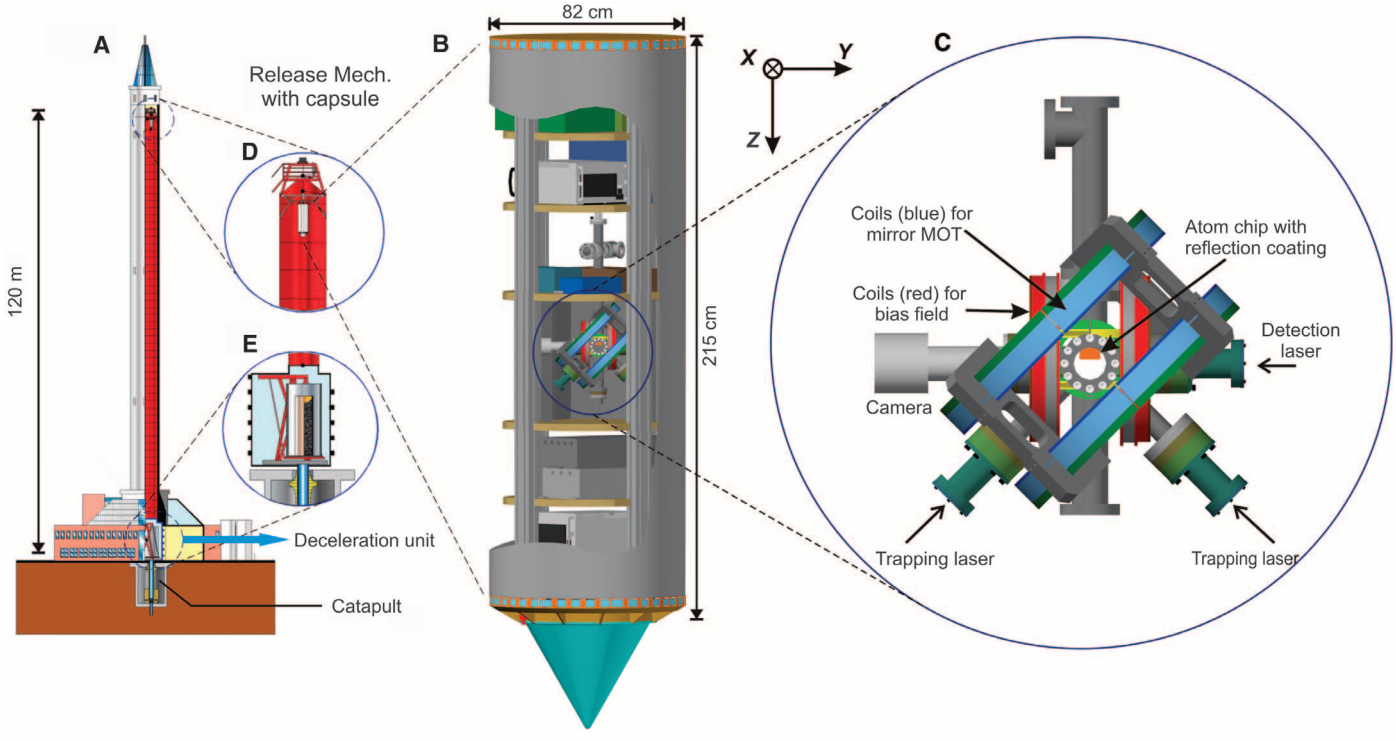

Fig. 1. Cuts through the ZARM drop tower facility in Bremen (**A**) and the capsule (**B**) containing the heart of the BEC experiment (**C**). The capsule is released from the top of the tower (**D**) and is recaptured after a free fall of 4.7 s through an evacuated stainless steel tube at the bottom of the tower by a 8-m-deep pool of polystyrene balls (**E**). In the process of recapturing the capsule, the experiment has to survive decelerations up to 500 m/s^2 (about 50 times the local gravitational acceleration). The facility permits up to three drops per day. The capsule contains all of the components necessary to prepare and observe a BEC, such as the laser systems for cooling the atoms, the ultrahigh-vacuum chamber with the atom chip, the current drivers and power supplies, a charge-coupled device (CCD) camera, and a control computer. The vacuum chamber is surrounded by two magnetic shields and allows us to include an atom interferometer in future experiments. Moreover, the catapult underneath the movable polystyrene pool offers the possibility of extending the time of free fall to 9 s.

macroscopic matter-wave packet, which provides us with a probe that is highly sensitive to magnetic and gravitational fields and represents a testing ground for physics at ultralow energy scales. We have performed more than 180 experiments to demonstrate the feasibility of coherent matter-wave experiments in microgravity (*4*), thus opening up a new avenue for high-precision measurements in space (*5*).

The drive for large expansion times of a BEC is motivated by the increase in sensitivity of an inertial sensor based on an atom interferometer with the square of the time (*6*) the atoms spend in the interferometer. As a result, cold atom–based sensors, such as gyroscopes or gravimeters (*7*), might reach an unprecedented sensitivity that is necessary to perform tests (*8*) of GR, such as the measurement (*9*, *10*) of the Lense-Thirring effect, which is a manifestation of gravitational forces induced by rotating masses (*11*). Moreover, recent advances in atom-optics technology have led to the preparation of tests of the equivalence principle with matter waves (*12*, *13*) rather than macroscopic systems, and these advances make the detection of gravitational waves feasible (*14*).

Unfortunately, the grip of gravity on matter makes it difficult in an Earth-bound laboratory to enable a BEC to expand freely over long periods. For example, during 1 s, a mass initially at rest would fall about 5 m. One way to circumvent this problem is levitation by electromagnetic forces counteracting gravity (*15*). However, only one class of atoms with specific magnetic properties or one species can be levitated at a time. This limitation serves as one motivating factor for our BEC experiment (*16*) in the drop tower (Fig. 1). Here, the complete apparatus is in free fall, and the capsule provides an environment with residual accelerations that are as low as 1 part in 10^5 of terrestrial gravity, conditions that are difficult to reach in other microgravity platforms.

The realization of this experiment required the miniaturization of the setup, which was made possible by the development of atom chips (*17*–*19*). We combined this technology with a mirror magneto-optical trap (MOT), which was loaded with roughly 1.3×10^7 atoms of ^{87}Rb from the background gas. Loading was completed after 10 s, and the capsule was then released. During the first second of free fall, the atoms are held in the mirror MOT until the initial vibrations of the capsule have damped out. The atoms are further cooled in optical molasses and transferred to an Ioffe-Pritchard trap on the chip. A BEC of about 10^4 atoms in the hyperfine state $F = 2$, $m_F = 2$ (where F and m_F are the quantum numbers for the total angular momentum and the Zeeman sublevel, respectively) is routinely obtained within 1 s after compression of the trap and radio frequency–induced evaporation. The lifetime of our condensate inside the trap is 3 s, which is longer than the remaining time of free fall. The temperature and chemical potential of the BEC are lowered by adiabatically opening the trap. Finally, the BEC is released by switching off the currents through the atom chip, which defines the origin of time for the expansion.

We observed the BEC by using the absorption imaging technique (Fig. 2A). As an example, we show in Fig. 2B a BEC after a time of flight of 100 ms in free fall. Even for this expansion time, the observation of a BEC in an Earth-bound laboratory becomes difficult, because one has to adiabatically lower the trap frequencies to reduce the mean field energy and, consequently, reduce the speed of expansion. It is at this point that microgravity becomes crucial, because it allows us to reach trap frequencies in the hertz regime, giving rise to ground-state energies of the atomic ensemble in the nanokelvin range.

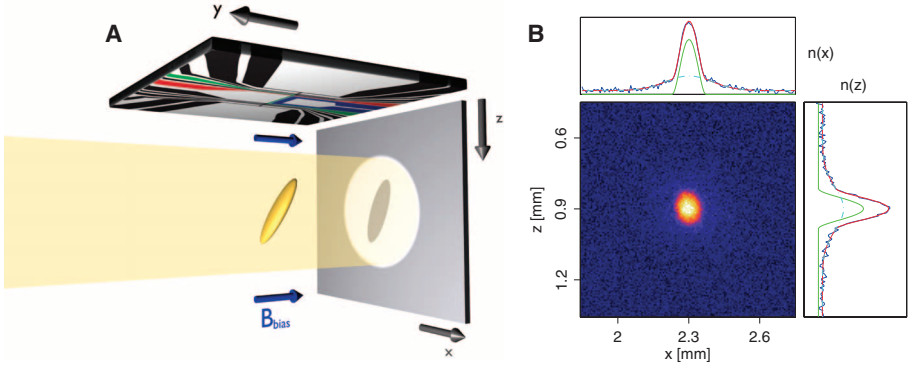

Fig. 2. Absorption imaging technique (**A**) used for the measurement of the two-dimensional spatial distribution of the BEC in microgravity (**B**). The BEC is initially confined by a combination of magnetic fields generated by the Z-shaped wire on the surface of the atom chip and a homogeneous bias field B_{bias}. After its release from the trap, the BEC is illuminated by a laser, and the shadow of the condensate is detected by a CCD camera (A). The resulting two-dimensional density distribution (B) corresponds to a BEC created and observed in free fall for an expansion time of 100 ms. Here, bright and dark colors indicate high and low atomic densities, respectively. At the top and on the right-hand side of this image, we show the x and z profiles, $n(x)$ and $n(z)$, of the integrated density distribution. Both consist of a central peak, representing the BEC, on top of a pedestal, formed by thermal atoms. A bimodal function (red line) is used to fit the BEC part and the thermal pedestal with the square of an inverted parabola (green line) and a Gaussian (blue line).

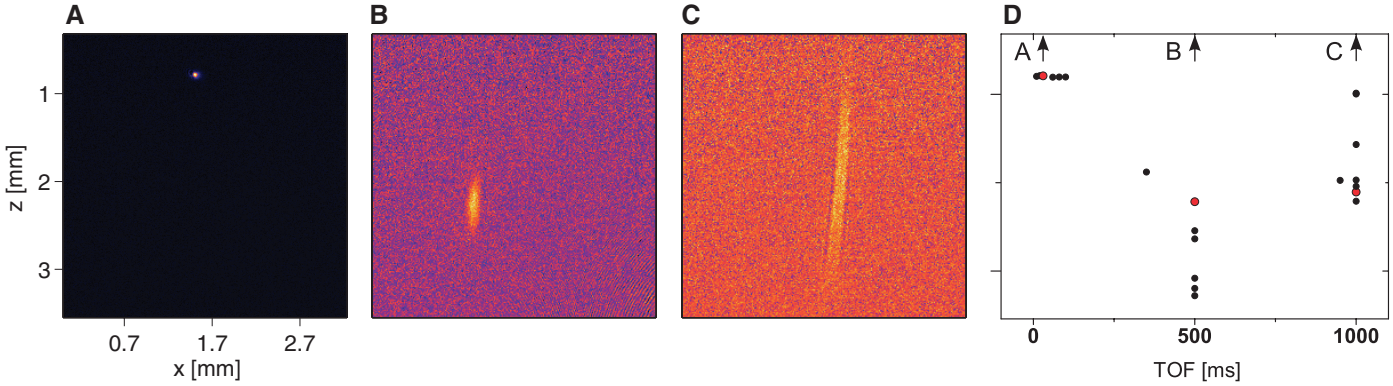

Fig. 3. Gallery of absorption images of BECs created and observed in free fall (**A** to **C**) together with the time dependence of the z coordinate of the center of mass of the BEC (**D**). The series starts with a time of flight of 30 ms (A), which is typical for Earth-bound laboratory experiments. The following two figures correspond to expansion times of 500 ms (B) and 1 s (C). In the latter case, the BEC extends over a distance of more than 2 mm in the z direction. In (D), we depict the z coordinates of the center of mass of more than 20 BECs as a function of the expansion time. The red dots correspond to the BECs presented in (A), (B), and (C). The z coordinate varies within a range of several millimeters, as discussed in (*23*).

In our experiment, the kinetic energy of the atoms is extremely low (9 nK), and the shadow of the BEC can even be observed after an expansion time of 1 s, when the BEC forms a delocalized wave packet extending over more than 2 mm.

In Figs. 3 and 4, we display the long-time evolution of a BEC during the extended free fall in the drop tower. Three absorption images corresponding to expansion times of 30 ms (Fig. 3A), 500 ms (Fig. 3B), and 1000 ms (Fig. 3C) are shown. The cases presented in Fig. 3, B and C, indicate a suppression of the expansion of the BEC in the x direction. Figure 3D shows that, during an evolution time of 1 s, the BEC moves within a range of about 3 mm in the z direction. Both effects, the suppression of the expansion and the motion of the center of mass, have their origins in the sensitivity of the BEC to any inhomogeneous stray magnetic fields during the expansion phase.

To provide a quantitative understanding of these observations, we compare and contrast in Fig. 4 the experimentally obtained half widths (solid squares) of the z and x profiles of the BEC with numerical simulations. The latter are based on scaling methods (*20*–*22*) and rely on a detailed modeling of the magnetic fields generated by the chip and the coils (*23*). The homogeneous stray field inside the vacuum chamber, which results, for example, from the vacuum pump, has been measured in the optical molasses phase in additional ground-based experiments. It is also included in the simulation, allowing us to estimate the trapping frequencies along the principal axes of the harmonic potential just before release to be 10, 22, and 27 Hz. We have also verified the validity of the scaling method by full three-dimensional simulations of the time-dependent Gross-Pitaevskii equation (*24*).

In the regime up to 100 ms (Fig. 4, A and C), which is at the limit of experiments in ground-based laboratories, both half widths display a systematic discrepancy between the observations (solid squares) and our simulations (black dashed curves) up to 75 ms. This deviation arises from a limitation in the optical resolution of the absorption imaging of the BEC, which we estimated to be approximately 20 μm. Taking this issue into account, our improved simulations (black solid curves) agree with the experimental observations.

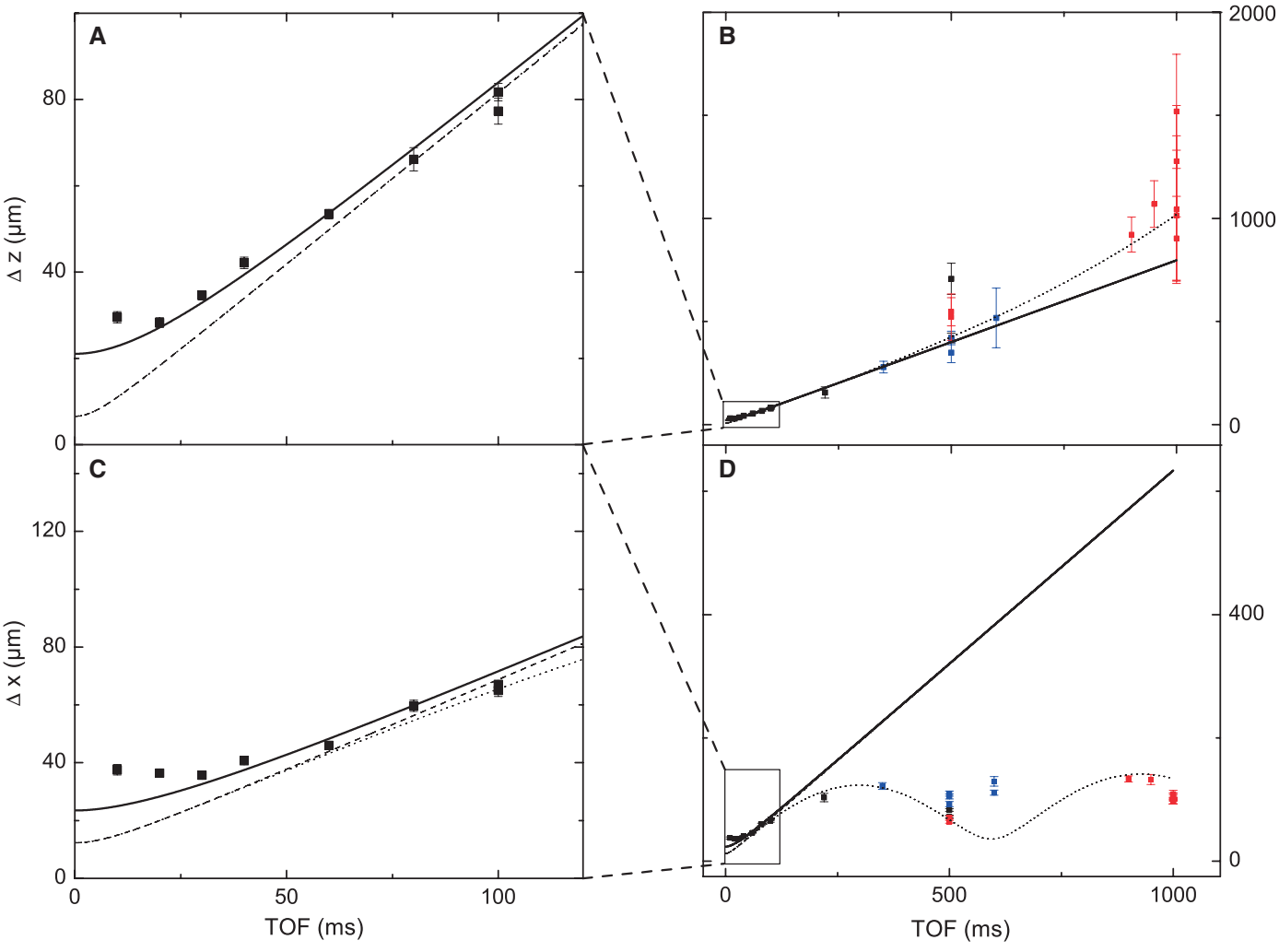

Fig. 4. Measured sizes of BECs in microgravity for short [(**A**) and (**C**)] and long [(**B**) and (**D**)] expansion times compared with numerical simulations. As a measure, we use the half widths Δz [(A) and (B)] and Δx [(C) and (D)] of the z and x profiles of the condensate extracted from the observed density distributions. The experimental data points (black, red, and blue solid squares) are shown with error bars due to density profile fittings; different colors indicate different detection configurations used in the absorption imaging of the BECs. Lines represent numerical simulations of the experiment based on the theory presented in (*20*–*22*) and summarized in (*23*). Up to 100 ms [(A) and (C)], the observed BEC sizes exceed the theoretical predictions (black dashed curves). By incorporating an estimated resolution limit of our optical imaging system of 20 μm, we find a good agreement between the corrected theoretical prediction (black solid curves) and the observed BEC sizes. For large expansion times [(B) and (D)], the observed expansion of the BEC does not obey the theoretically predicted linear growth for a vanishing magnetic field (black solid curves). However, by taking weak field curvatures of less than 1 $\mu T/mm^2$ into account, our simulations (black dotted curves) allow for a qualitative explanation of the observed data points.

Microgravity enables us to venture into the regime of unprecedented long time evolution of the BEC up to 1 s (Fig. 4, B and D) with our setup. Our measurements reveal the above-mentioned suppression of the expansion in the x direction. Although our theory (black solid curves) predicts a linear growth, we observe a saturation. In addition, the observed widths in the z direction are larger than expected.

The origin of both deviations can be traced back to the fact that, during the expansion phase, the atoms are in the $F = 2$, $m_F = 2$ hyperfine state. Because of the long expansion times, these deviations represent a sensitive probe of tiny magnetic field gradients and curvatures. By including magnetic field curvatures on the order of a few microtesla per square millimeter in our simulation (black dotted curves), we are able to provide a qualitative explanation of the observed half widths. A coherent transfer of the BEC into the magnetically insensitive hyperfine state $F = 2$, $m_F = 0$ would avoid the influence of parasitic effects, and the implementation of this transfer is currently under way.

We anticipate a multitude of new research directions for ultracold, dilute quantum gases in free fall. A spin-off from our experiment is the possibility of preparing an extremely dilute wave packet at the lowest energy scales. This limit is difficult to reach in standard BEC experiments but is relevant for the observation of quantum reflection (*25*) or Anderson localization (*26*, *27*). Future atom interferometers in space will probe the boundary between GR and QM.

References and Notes

1. C. W. Misner, K. S. Thorne, J. A. Wheeler, *Gravitation* (Freeman, San Francisco, 1973).
2. E. A. Cornell, C. E. Wieman, *Rev. Mod. Phys.* **74**, 875 (2002).
3. W. Ketterle, *Rev. Mod. Phys.* **74**, 1131 (2002).
4. G. Stern *et al.*, *Eur. Phys. J. D* **53**, 353 (2009).
5. E. Arimondo, W. Ertmer, W. P. Schleich, E. M. Rasel, Eds., *Proceedings of the International School of Physics "Enrico Fermi" Course CLXVIII "Atom Optics and Space Physics"* (IOS Press, Bologna, Italy, 2009).
6. P. R. Berman, Ed., *Atom Interferometry* (Academic Press, San Diego, CA, 1997).
7. A. Peters, K. Y. Chung, S. Chu, *Nature* **400**, 849 (1999).
8. W. P. Schleich, M. O. Scully, in *New Trends in Atomic Physics, Proceedings of the Les Houches Summer School 1982, Session XXXVIII*, G. Grynberg, R. Stora, Eds. (North-Holland, Amsterdam, 1984), pp. 995–1124.
9. I. Ciufolini, E. C. Pavlis, *Nature* **431**, 958 (2004).
10. I. Ciufolini, *Nature* **449**, 41 (2007).
11. I. Ciufolini, J. A. Wheeler, *Gravitation and Inertia* (Princeton Univ. Press, Princeton, NJ, 1995).
12. S. Fray, C. Alvarez Diez, T. W. Hänsch, M. Weitz, *Phys. Rev. Lett.* **93**, 240404 (2004).
13. S. Dimopoulos, P. W. Graham, J. M. Hogan, M. A. Kasevich, *Phys. Rev. Lett.* **98**, 111102 (2007).
14. S. Dimopoulos, P. W. Graham, J. M. Hogan, M. A. Kasevich, S. Rajendran, *Phys. Rev. D Part. Fields Gravit. Cosmol.* **78**, 122002 (2008).
15. A. E. Leanhardt *et al.*, *Science* **301**, 1513 (2003).
16. A. Vogel *et al.*, *Appl. Phys. B* **84**, 663 (2006).
17. W. Hänsel, P. Hommelhoff, T. W. Hänsch, J. Reichel, *Nature* **413**, 498 (2001).
18. R. Folman, P. Krüger, J. Schmiedmayer, J. Denschlag, C. Henkel, *Adv. At. Mol. Opt. Phys.* **48**, 263 (2002).
19. J. Fortágh, C. Zimmermann, *Rev. Mod. Phys.* **79**, 235 (2007).
20. Y. Kagan, E. L. Surkov, G. V. Shlyapnikov, *Phys. Rev. A* **54**, R1753 (1996).
21. Y. Castin, R. Dum, *Phys. Rev. Lett.* **77**, 5315 (1996).
22. P. Storey, M. Olshanii, *Phys. Rev. A* **62**, 033604 (2000).
23. Materials and methods are available as supporting material on *Science* Online.
24. G. Nandi, R. Walser, E. Kajari, W. P. Schleich, *Phys. Rev. A* **76**, 063617 (2007).
25. T. A. Pasquini *et al.*, *Phys. Rev. Lett.* **97**, 093201 (2006).
26. J. Billy *et al.*, *Nature* **453**, 891 (2008).
27. G. Roati *et al.*, *Nature* **453**, 895 (2008).

28. This project is supported by the German Space Agency Deutsches Zentrum für Luft- und Raumfahrt (DLR) with funds provided by the Federal Ministry of Economics and Technology (BMWi) under grant number DLR 50 WM 0346. We thank the German Research Foundation for funding the Cluster of Excellence QUEST Centre for Quantum Engineering and Space-Time Research.

Supporting Online Material

www.sciencemag.org/cgi/content/full/328/5985/1540/DC1
Materials and Methods
References

5 March 2010; accepted 10 May 2010
10.1126/science.1189164

Hot-Electron Transfer from Semiconductor Nanocrystals

William A. Tisdale,[1] Kenrick J. Williams,[2,3]* Brooke A. Timp,[2] David J. Norris,[1]† Eray S. Aydil,[1]† X.-Y. Zhu[2,3]*†

In typical semiconductor solar cells, photons with energies above the semiconductor bandgap generate hot charge carriers that quickly cool before all of their energy can be captured, a process that limits device efficiency. Although fabricating the semiconductor in a nanocrystalline morphology can slow this cooling, the transfer of hot carriers to electron and hole acceptors has not yet been thoroughly demonstrated. We used time-resolved optical second harmonic generation to observe hot-electron transfer from colloidal lead selenide (PbSe) nanocrystals to a titanium dioxide (TiO_2) electron acceptor. With appropriate chemical treatment of the nanocrystal surface, this transfer occurred much faster than expected. Moreover, the electric field resulting from sub–50-femtosecond charge separation across the PbSe-TiO_2 interface excited coherent vibrations of the TiO_2 surface atoms, whose motions could be followed in real time.

The maximum theoretical efficiency of a standard silicon solar cell in use today is limited to ~31%, in part by the loss of any photon energy that exceeds the semiconductor bandgap (*1*). Absorption of high-energy photons creates hot electrons and holes that cool quickly (within ~1 ps) to the band edges by sequential emission of phonons. There the carriers remain for hundreds of picoseconds or longer before slower processes such as radiative or nonradiative recombination occur. The goal of standard solar cells is to extract these band-edge electrons and holes to produce electrical current. However, because of the initial cooling process, a substantial amount of solar energy has already been irreversibly lost. If instead, all of the energy of the hot carriers could be captured, solar-to-electric power conversion efficiencies could be increased, theoretically to as high as 66% (*2*). We can envision the realization of such a hot carrier solar cell in a semiconductor device where scattering among photoexcited electrons and reabsorption of additional photons in the conduction band is faster than hot-electron cooling, resulting in a quasi-equilibrium characterized by an electron temperature much higher than the lattice temperature. This is coupled with equally fast hot-electron transfer to an electron conductor in a narrow energy window (to minimize additional energy loss in the latter). The same argument applies to the holes.

A potential route to the above hot carrier solar cell is to use semiconductor nanocrystals, or quantum dots (*3*). In these materials, the quasi-continuous conduction and valence energy bands of the bulk semiconductor become discretized owing to confinement of the charge carriers. Consequently, the energy spacing between the electronic levels can be much larger than the highest phonon frequency of the lattice, creating a "phonon bottleneck" in which hot-carrier relaxation is only possible via slower multiphonon emission (*4*). For example, hot-electron lifetimes as long as ~1 ns have been

[1]Department of Chemical Engineering and Materials Science, University of Minnesota, Minneapolis, MN 55455, USA. [2]Department of Chemistry, University of Minnesota, Minneapolis, MN 55455, USA. [3]Department of Chemistry and Biochemistry, University of Texas, Austin, TX 78712, USA.

*Present address: Department of Chemistry and Biochemistry, University of Texas, Austin, TX 78712, USA.
†To whom correspondence should be addressed: zhu@cm.utexas.edu (X.-Y.Z.), dnorris@umn.edu (D.J.N.), aydil@umn.edu (E.S.A.)

ERRATUM

Post date 2 July 2010

Reports: "Bose-Einstein condensation in microgravity" by T. van Zoest *et al*. (18 June, p. 1540). J. Reichel's affiliation was listed incorrectly. Affiliation 9 should be: Laboratoire Kastler-Brossel de l'Ecole Normale Supérieure, Université Pierre et Marie-Curie-Paris 6, CNRS, 24 rue Lhomond, 75005 Paris, France.